



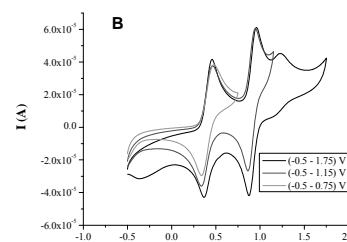
COMPARATIVE ELECTROCHEMICAL STUDY OF 2,2-DIPHENYL-1-(2,6-DINITRO-4-TRIFLUOROMETHYLPHENYL)HYDRAZINE AND 2,2-DI-*p*-TOLYL-1-(2,4,6-TRINITROPHENYL)HYDRAZINE

Cassiana Cristina ANDREI, Laura SĂRDAN, Sorana IONESCU, Daniela BALA and Constantin MIHAILCIUC*

Physical Chemistry Department, Faculty of Chemistry, University of Bucharest, 4-12 Regina Elisabeta, 030018 Bucharest, Roumania

Received March 7, 2014

The CV and DPV behaviour is investigated for two hydrazine derivatives, 2,2-di-*p*-tolyl-1-(2,4,6-trinitrophenyl)hydrazine (A), and 2,2-diphenyl-1-(2,6-dinitro-4-trifluoromethylphenyl)hydrazine (B) which differ structurally by the presence in compound B both of a very efficient electron-withdrawing group (trifluoromethyl) in position 4 of the 2,4-dinitrophenyl moiety (instead of the nitro group from similar position in compound A) and of phenyl groups instead of tolyl groups in compound A. The acidic hydrogen atom, bonded to a nitrogen atom, can be removed by using a proton abstractor like the methoxide ion base. So that for each compound the experiment may be conducted in the absence and in the presence of this hydrogen abstractor. In each case a mechanism of the electrode reaction is proposed. The behaviour of each compound depends upon the electronic conjugation (electron withdrawing and electron donating moieties being present in their structures) leading to similar and/or different CV and DPV features. The anodic and cathodic peak potentials, the half-wave potentials, the shape factor and the peak separation are involved in the electrochemical mechanisms description. A mechanism for the three oxidation steps involved is proposed and confirmed by quantum chemical calculations.



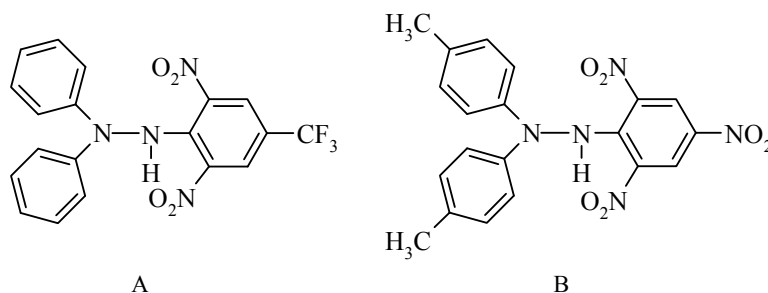
INTRODUCTION

The interest for some new organic free stable radicals increased rapidly in the past years because of their many applications in different domains. For instance, such compounds are interesting in producing materials with magnetic properties.¹⁻⁴ The most well known free radical derived from hydrazine is DPPH (2,2-diphenyl-1-picrylhydrazyl) synthesized by Goldschmidt in 1922.⁵ It is characterised by chemical stability, colour changing properties depending on the pH of the media, and it is also a good hydrogen- or electron-abstractor.⁶ Due to its properties it has been used as scavenger for many

other radicals, as standard in ESR spectroscopy, but also as indicator for measuring the antioxidant capacity in human plasma.^{7,8}

Taking as a model the DPPH many other similar compounds were synthesised. In this paper we study electrochemical behaviour of two compounds: 2,2-diphenyl-1-(2,6-dinitro-4-trifluoromethylphenyl)hydrazine (A), and 2,2-di-*p*-tolyl-1-(2,4,6-trinitrophenyl)hydrazine (B) (Scheme 1). In order to obtain detailed information concerning the redox processes of these hydrazine-derivatives, cyclic voltammetry (CV) and differential pulse voltammetry (DPV) measurements were performed. Another two similar compounds were already studied in a previous paper.⁹

* Corresponding author: cmpaul@gw-chimie.math.unibuc.ro



Scheme 1 – Structure of compounds: 2,2-diphenyl-1-(2,6-dinitro-4-trifluoromethylphenyl)hydrazine (A), and 2,2-di-*p*-tolyl-1-(2,4,6-trinitrophenyl)hydrazine (B).

EXPERIMENTAL

Apparatus: Electrochemical experiments were performed with a potentiostat-galvanostat system Autolab PGStat 12 controlled by General Purpose Electrochemical System (GPES) electrochemical interface for Windows (version 4.9.007). Three electrodes in one-compartment cell (10 mL) were used in all experiments: two disk-shaped platinum electrodes (Metrohm, 3 mm in diameter) as working electrode and counter electrode, respectively and Ag (wire) as pseudo-reference electrode.

The platinum electrode surfaces were polished with alumina slurry on a polishing pad, washed with distilled water and sonicated for 1 minute.

Chemicals: Compounds 2-diphenyl-1-(2,6-dinitro-4-trifluoromethylphenyl)hydrazine (A) and 2,2-di-*p*-tolyl-1-(2,4,6-trinitrophenyl)hydrazine (B), were prepared as described.^{10,11} The other reagents: acetonitrile (Fisher Chemicals), Bu_4NBF_4 (Fluka), sodium hydroxide (Sigma), methanol (Chimpar) were used as purchased.

Measurements: Two working solutions of 10 mL each were prepared and studied: one obtained by dissolving the electroactive compounds A or B (1 mM) in acetonitrile with 0.1 M Bu_4NBF_4 as supporting electrolyte, and the other by adding 0.1 mL NaOH 0.11 M in methanol to the former solution in order to create a basic medium (the obtained effect was the hydrogen-atom abstraction from hydrazyl moiety). CV and DPV measurements were then performed.

For both compounds cyclic voltammetry experiments were carried out in the potential ranges: from -0.50 V to +1.85 V, from -0.50 V to +0.75 V and, respectively, from -0.50 V to +1.20 V. To investigate the influence of scan rate several values were used in the range between 0.05 to 0.75 V s^{-1} . DPV curves were recorded on the same potential domains using different parameters: step potential 10 mV, and two values for modulation amplitude 25 and 50 mV, respectively.

The solution containing the electroactive hydrazine derivative and the supporting electrolyte, either without or with methoxide ion, was purged with Ar, and low pressure inert gas atmosphere was maintained above the solution during the electrochemical experiments.

The quantum chemical calculations were made with the Gaussian09 program¹² using the DFT method with a B3LYP functional^{13,14} and the TZVP basis set.¹⁵ The vertical, Ev, and adiabatic, Ea, energies of several possible oxidation processes of the form $\text{Red} \leftrightarrow \text{Ox} + e^-$ were computed as $E_{\text{Ox}} - E_{\text{Red}}$, in order to be correlated to the experimental oxidation potential

from cyclic voltammetry. The solvent, acetonitrile, was modelled as a polarizable continuum in the frame of the PCM model.¹⁶

RESULTS AND DISCUSSION

Electrochemical study of (A) 2,2-diphenyl-1-(2,6-dinitro-4-trifluoromethylphenyl)hydrazine and (B). 2,2-di-*p*-tolyl-1-(2,4,6-trinitrophenyl)hydrazine without methoxide ion added

Fig. 1 shows the cyclic voltammetry behaviour of 2,2-diphenyl-1-(2,6-dinitro-4-trifluoromethylphenyl) hydrazine (1 mM) (Fig. 1A) and 2,2-di-*p*-tolyl-1-(2,4,6-trinitrophenyl) hydrazine (1 mM) (Fig. 1B), for scan rates between 0.05 V s^{-1} and 0.75 V s^{-1} and the potential range between -0.5 V and 1.85 V. The voltammograms are characterised by a complex morphological aspect that indicates a multistep oxidation-reduction electrode reaction and protonation-deprotonation chemical reaction which intervene in the last electron transfer.

For the compound A at small scan rates four anodic peaks (ap_1 , ap_2 , ap_3 , ap_4) can be observed. When the scan rate becomes superior to 0.1 $\text{V} \cdot \text{s}^{-1}$ the fourth anodic peak is no more observable (the third anodic peak merges with the fourth one because the distance between them on the potential scale is too small). So that, at high scan rates only 3 anodic peaks (ap_1 , ap_2 , ap_{3-4}) can be observed at the potential values: 0.333 V, 0.980 V and 1.254 V. The cyclic voltammograms present two cathodic peaks (cp_1 and cp_2) as well appearing at the potential values of 0.280 V and 0.912 V, respectively. A shoulder around -0.300V can also be observed but it may be due to an insufficient purging with argon. Comparing the voltammograms of compound A and of the compound B a difference between the anodic

waves can be emphasised. The compound B shows only three anodic peaks no matter the scan rate (appearing at the potential values: 0.455V, 0.953V and 1.243V). It can be observed that the third anodic peak in this case becomes a shoulder at high scan rates. The voltammograms are not keeping the same allure from small scan rates to high scan rates. The compound B shows also 2 cathodic peaks as observed for the compound A (appearing at 0.369V and 0.877 V).

The genetic link between anodic and cathodic peaks was proved by CV studies on two narrower potential domains (between -0.50 V and +0.75 V and respectively between -0.50 V and +1.20 V). The voltammograms obtained were compared with the voltammogram measured for the main potential domain considered. Fig. 2 shows the voltammograms obtained considering the three potential domains and a particular scan rate of $0.5 \text{ V} \cdot \text{s}^{-1}$.

Thus, for both compounds the anodic peak 1 is genetically linked with the cathodic peak 1 and the anodic peak 2 is genetically linked with the cathodic peak 2. The experiment was made also using DPV in the same conditions and considering 3 different potential domains. Comparing the DP-Voltammograms (scan rate chosen 0.05 V/s), not shown here, we arrived at the same conclusion and we confirmed the results obtained by CV.

Using the values corresponding to peak potentials we can calculate for each recorded peak the half-wave potential, $E_{1/2} = \frac{E_{pa} + E_{pc}}{2}$, the peak-to-peak separation, $\Delta E_p = E_{pa} - E_{pc}$ and the shape factor¹¹, $E_p - E_{p/2}$ (see Table 1). Considering the shape factor, all three electron transfers are essentially single-electron processes and the behaviour of the first two electrode reactions is near the reversible case.

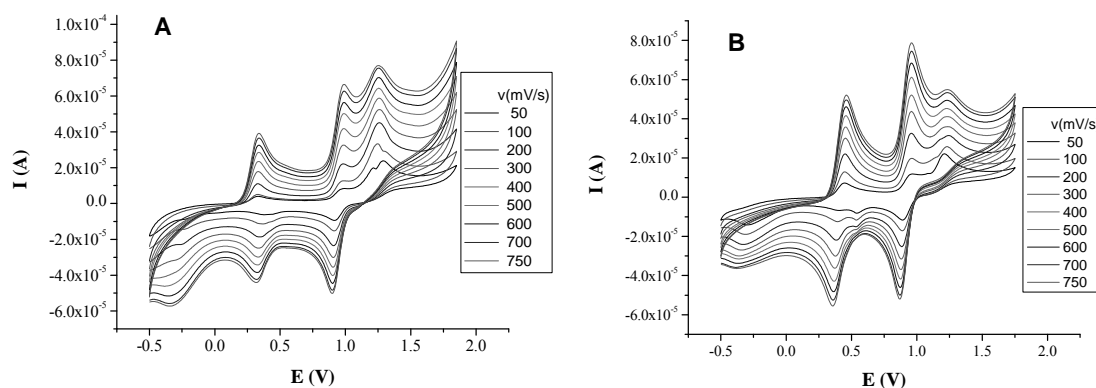


Fig. 1 – Cyclic voltammograms of (A) 2,2-diphenyl-1-(2,6-dinitro-4-trifluoromethylphenyl)hydrazine (0.001 M) in acetonitrile/ Bu_4NBF_4 (0.1M) and (B) 2,2-di-*p*-tolyl-1-(2,4,6-trinitrophenyl)hydrazine- graph B (0.001 M) in acetonitrile/ Bu_4NBF_4 (0.1M), potential domain (-0.50 V --- +1.85 V), scan rates between 0.05 and 0.75 V s^{-1} .

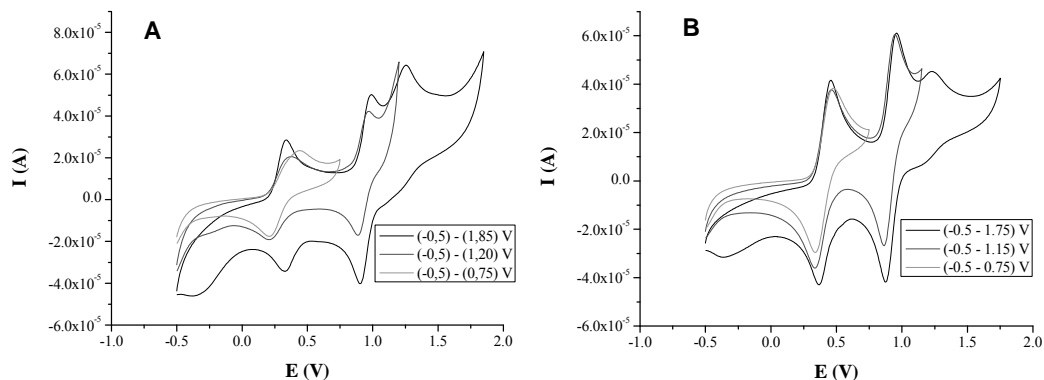


Fig. 2 – Cyclic voltammograms of (A) 2,2-diphenyl-1-(2,6-dinitro-4-trifluoromethylphenyl)hydrazine (0.001 M) in acetonitrile/ Bu_4NBF_4 (0.1 M) and (B) 2,2-di-*p*-tolyl-1-(2,4,6-trinitrophenyl)hydrazine (0.001 M) in acetonitrile/ Bu_4NBF_4 (0.1 M), for different potential domains, scan rate 0.5 V s^{-1} .

Table 1

Main electrochemical data for 2,2-diphenyl-1-(2,6-dinitro-4-trifluoromethylphenyl) hydrazine and 2,2-di-*p*-tolyl-1-(2,4,6-trinitrophenyl)hydrazine in the absence of methoxide ion

Compound	E_{pa1}	$E_p - E_{p/2}$	E_{pa2}	$E_p - E_{p/2}$	E_{pa3}	$E_p - E_{p/2}$
(A)	0.333	0.061	0.984	0.059	1.254	0.073
(B)	0.455	0.066	0.953	0.053	1.243	0.066
	E_{pc1}	$E_p - E_{p/2}$	E_{pc2}	$E_p - E_{p/2}$		
(A)	0.330	0.067	0.906	-0.057		
(B)	0.369	-0.059	0.877	-0.058		

Table 2

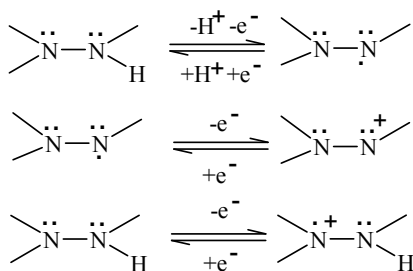
Parameters characterising the plots I_p vs. $v^{1/2}$ for both compounds

Compound A			
Peak	I_p	R	SD
ap ₁	$I_{pa} = 1.416 \cdot 10^{-6} + 2.471 \cdot 10^{-5} v^{1/2}$	0.975	$1.366 \cdot 10^{-6}$
cp ₁	$I_{pc} = 3.24 \cdot 10^{-6} - 1.95 \cdot 10^{-5} v^{1/2}$	0.996	$4.540 \cdot 10^{-7}$
ap ₂	$I_{pa} = -2.810 \cdot 10^{-6} + 3.757 \cdot 10^{-5} v^{1/2}$	0.990	$1.305 \cdot 10^{-6}$
cp ₂	$I_{pc} = 3.71 \cdot 10^{-6} - 4.01 \cdot 10^{-5} v^{1/2}$	0.998	$1.120 \cdot 10^{-7}$
Compound B			
Peak	I_p	R	SD
ap ₁	$I_{pa} = 4.66 \cdot 10^{-6} + 4.98 \cdot 10^{-5} v^{1/2}$	0.998	$5.290 \cdot 10^{-7}$
cp ₁	$I_{pc} = 9.691 \cdot 10^{-6} - 7.132 \cdot 10^{-5} v^{1/2}$	0.999	$5.923 \cdot 10^{-7}$
ap ₂	$I_{pa} = -6.41 \cdot 10^{-6} + 5.24 \cdot 10^{-5} v^{1/2}$	0.997	$8.962 \cdot 10^{-7}$
cp ₂	$I_{pc} = 1 \cdot 10^{-5} - 5.596 \cdot 10^{-5} v^{1/2}$	0.999	$2.687 \cdot 10^{-7}$

The values obtained for the shape factor are situated around 0.059 V (between 0.053 and 0.073) for both compounds. Considering this values but also the peak separation (0.003V for the first couple of peaks or 0.078V for the second one corresponding to compound A or 0.086V for the first couple of peaks or 0.076V for the second one corresponding to compound B) we can prove the reversibility of the first and the second electron transfer processes for each of two compounds A and B. Also, the plots I_{pa} vs. $v^{1/2}$ and I_{pc} vs. $v^{1/2}$, respectively, leading to straight lines (parameters shown in Table 2), confirm the reversibility of the couple of peaks aforementioned for both compounds. As concerns the third process involved, it is an EC mechanism type. Taking into account the heights of the peaks one can say that each reaction involves one electron transfer.

Comparing the position of the anodic peak potentials for compounds A and B, it is obvious that the first oxidation event occurs easier for A than for B. This is due to the presence of more strongly deactivating nitro group in position 4 in B instead of trifluoromethyl in the same position 4 in A. The effect is that the electron density on N1 atom is lower in B than in A. As concerns the electron transfer at N2 atom, the presence of methyl radicals in positions 4' and 4'', with electron donating effect, rises even if very little the electron density at N2 atom and, for this reason, the oxidation at N2 atom occurs easier in B than in A. The second electron transfer at N1 atom takes place practically at the same anodic potential, therefore as easy.

As concerns the mechanism of the electrode reaction in the absence of methoxide ion, the following reaction steps (Scheme 2) might be proposed:



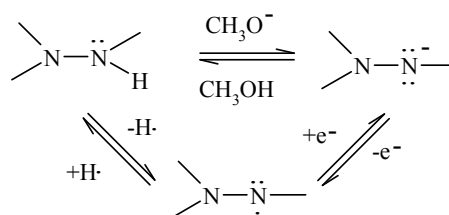
Scheme 2 – Reaction mechanism proposed for hydrazine moiety electrochemistry in the absence of methoxide ion.

The first couple of peaks, characterised by $E_{1/2} = 0.331$ V for the compound A and $E_{1/2} = 0.412$ V for the compound B, corresponds to the first electron transfer represented in Scheme 2 which involves besides an electron transfer a deprotonation-protonation process. The presence of the three NO_2 groups in the picryl fragment determines a weak acidic character of the hydrazine group, even in aprotic solvents, as reported in the literature, *i.e.* diphenylpicrylhydrazine has $\text{pK}_a = 5.9$ in DMSO.¹⁷ On the other hand, the proton abstraction in the NH group was also reported for 1,3,7,9-tetranitrophenothiazine-5-oxide in dimethylformamide,¹⁸ for which the EPR spectrum of the negative radical-ion electrolytically obtained does not present the splitting corresponding to this proton. This is why at least for compound B a non-concerted deprotonation step followed by the electron transfer may be taken into account. These electron transfer and deprotonation-protonation processes are located at the nitrogen numbered with 1 in hydrazyl moiety. The second couple of peaks, characterised by $E_{1/2} = 0.945$ V for A and $E_{1/2} = 0.915$ V for B, appears as consequence of an electron transfer occurring on the same initial hydrazine but at the tertiary nitrogen (numbered with 2) of the hydrazyl moiety. The result is the formation of the nitrogen cation at the tertiary nitrogen (numbered with 2) of the hydrazyl moiety. The third anodic peak occurring at $E_{\text{pa}_3} = 1.254$ V for A and $E_{\text{pa}_3} = 1.243$ V for B is given by a second electron transfer which can take place after the first electron transfer at N1 atom and leading to the nitrogen cation at the nitrogen numbered with 1. This anodic peak is not accompanied by a cathodic counterpeak, the mechanism being an EC mechanism, possibly due to deprotonation of the hydrazine cation, which generates the stable hydrazyl radical. The third electron transfer occurs at the secondary nitrogen

atom (N1 atom). The above mechanism of the entire electrode reaction is located on the hydrazyl moiety. The assignment of the first and third peaks was based on interpretation of the behaviour of similar compounds,^{19,20} and will be further discussed on grounds of the quantum chemical calculations results.

Electrochemical study of (A) 2,2-diphenyl-1-(2,6-dinitro-4-trifluoromethylphenyl)hydrazine and (B). 2,2-di-*p*-tolyl-1-(2,4,6-trinitrophenyl)hydrazine with methoxide ion added

The hydrazyl moiety of the compound is characterized by acidity of the NH group which is able to lose the proton in basic media as shown in Scheme 3 – horizontally. It can also lead to a radical in one-step process (left side) by directly losing the hydrogen atom or in a two-step process losing at first the proton in an acid-base process, and then losing an electron (right side). This is the reason why we realised the electrochemical study of the compounds also in basic media (in the presence of methoxide ion).



Scheme 3 – Generic mechanism illustrating the redox and acidic-basic behaviour of hydrazine moiety.

In order to create a basic media, 100 μL of 0.11 M NaOH in methanol (solution containing methoxide ion) has been added to the solution of 2,2-diphenyl-1-(2,4-dinitrophenyl)hydrazine 0.001M (or 2,2-di-*p*-tolyl-1-(2,4,6-trinitrophenyl)hydrazine 0.001M) in acetonitrile.

Fig. 3 illustrates the comparative voltammograms obtained for two different conditions already discussed: one by using the solution of each compound dissolved in acetonitrile and another one using the same solution but with 0.11 M solution of sodium methoxide added.

In the presence of the methoxide ion as deprotonating agent, a cathodic shift of all anodic peaks is recorded for both compounds. A decrease (shift towards more cathodic values of the potential) of the peak potentials for the oxidation of nitrogen from

NH-group (N1 atom) firstly at nitrogen radical (first anodic wave) and secondly at nitrogen cation from the nitrogen radical (third anodic wave), and then for the oxidation of tertiary nitrogen (N2 atom) at nitrogen cation (second anodic wave) is observed. Regarding the second wave, the de-electronation reaction occurring at tertiary nitrogen from hydrazyl moiety involves the more stabilized lone pair of electrons due to its participation to two different conjugation processes with phenyl groups. As a consequence, the de-electronation process takes place at a more anodic potential.

The electron transfer processes are preceded by a proton extraction as a consequence of the addition of the methoxide ion in the media, so the first two steps are not concerted. For compound A the first couple of peaks (characterised by $E_{1/2}=0.285$ V), is given by the first electron transfer in Scheme 4. A comparison with the mechanism in Scheme 2 reveals that the last two oxidation steps are similar in the absence and presence of methoxide and that in the hypothesis of

non-concerted proton transfer followed by the electron transfer in Scheme 2 all the electron transfer processes are similar in the absence and presence of methoxide for compound B.

The anodic peak occurring at approximately $E_{pa_3}=1.181$ V corresponds to the second electron transfer in Scheme 4 and leads to the formation of the nitrogen cation at N1 atom. This anodic peak has now the appearance of a shoulder and its cathodic counterpeak is almost absent in the CV study but very visible in the DPV study. A third electron transfer occurs at the tertiary nitrogen atom (N2 atom) and appears at $E_{1/2}=0.886$ V.

Table 3 summarizes the differences appeared in the peak potential positions in the absence and in the presence of the methoxide ion. All the peak potentials are cathodically shifted in the presence of the methoxide the electron abstraction being more favourable.

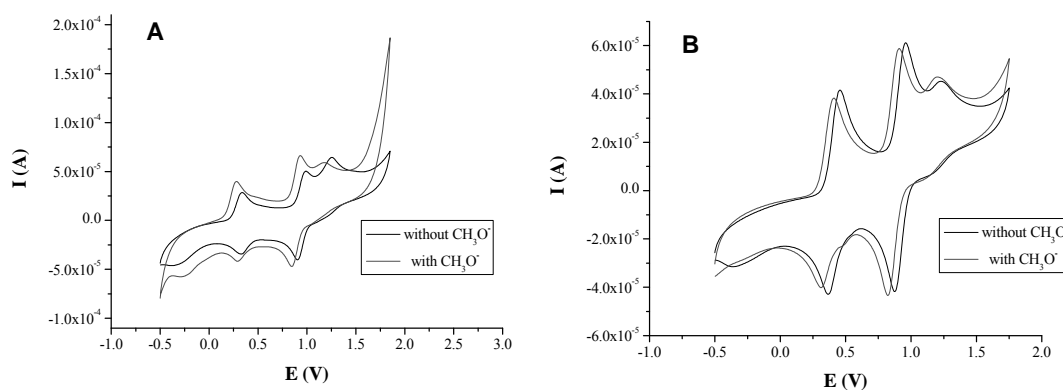
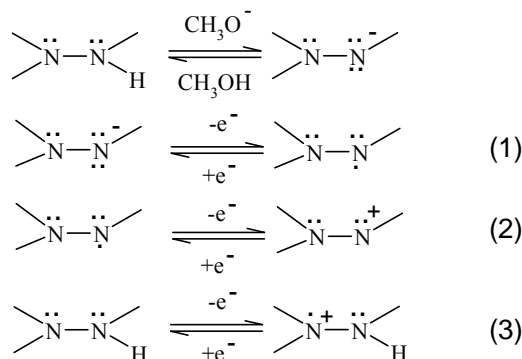


Fig. 3 – Cycling voltammograms of (A) 2,2-diphenyl-1-(2,6-dinitro-4-trifluoromethylphenyl)hydrazine (0.001 M) and (B) 2,2-di-*p*-tolyl-1-(2,4,6-trinitrophenyl)hydrazine with (blue) or without (red) methoxide ion added, potential domain (-0.50 V --- +1.85 V), scan rate 0.5 Vs⁻¹.



Scheme 4 – Reaction mechanism proposed for hydrazine moiety electrochemistry in the presence of methoxide ion.

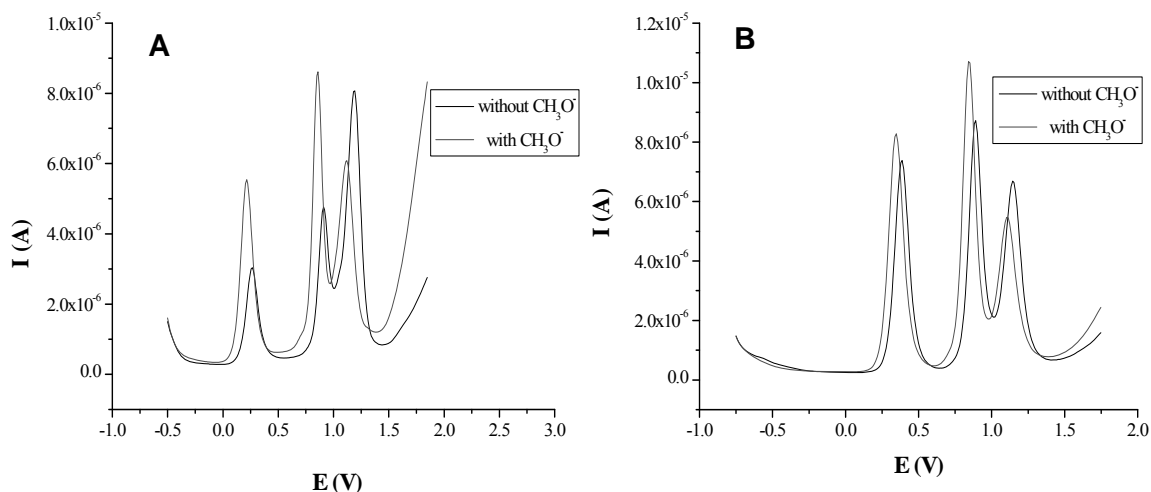


Fig. 4 – DPV traces of (A) 2,2-diphenyl-1-(2,6-dinitro-4-trifluoromethylphenyl)hydrazine (0.001 M) in acetonitrile/ Bu_4NBF_4 (0.1 M) and (B) 2,2-di-*p*-tolyl-1-(2,4,6-trinitrophenyl)hydrazine (0.001 M) in acetonitrile/ Bu_4NBF_4 (0.1 M) with (blue) or without (red) methoxide ion added, potential domain (0.0 V --- + 1.75 V), DPV parameters being $\text{SP}=10$ mV and $\text{MA}=25$ mV.

Table 3

The displacement of peaks recorded using DPV technique for the compounds A and B in absence and in presence of methoxide ion in the media

E_{pa} (V)	Compound A			Compound B		
	ap_1	ap_2	ap_3	ap_1	ap_2	ap_3
$E_{\text{pa, no CH}_3\text{O}^-}$	0.265	0.910	1.192	0.388	0.892	1.143
$E_{\text{pa, with CH}_3\text{O}^-}$	0.215	0.860	1.121	0.348	0.841	1.113
$\Delta E_{\text{pa}} = E_{\text{pa, no CH}_3\text{O}^-} - E_{\text{pa, with CH}_3\text{O}^-}$	0.050	0.050	0.071	0.040	0.051	0.030

The DPV study of both compounds in the absence and in the presence of methoxide ion in the media confirms the behaviour observed using CV technique but also helps to find the specific values of the three anodic peak potentials. These values permit to calculate the displacements recorded for each compound in different media used (as shown in Table 3).

Fig. 4 confirms the cathodic shift of the peak potentials in the presence of methoxide ion comparing to the absence of methoxide ion. Thus it can be emphasised that the oxidative processes occur easier (at lower values of the anodic potentials) for the deprotonated derivative than for the protonated derivative. For compound B, the similarity of the mechanism of the first oxidation step in the absence and presence of the methoxide ion cannot be excluded, i.e. the non-concerted nature of the deprotonation and electron transfer processes.

Quantum chemical calculations

Quantum chemical calculations were performed on compound B in order to shed some light on the

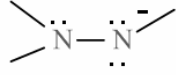
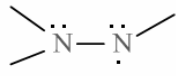
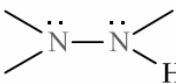
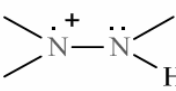
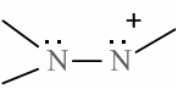
mechanism of the electrochemical processes. Only the non-concerted deprotonation-electron transfer processes as the first oxidation step were taken into account (as in Scheme 3). The experimental values of the oxidation potentials are considered to increase in the same order as the computed energy of the respective process noted as (1), (2), (3) in Scheme 3, E_v or E_a . The results of the DFT calculations are presented in Table 4. Looking at the energy of the HOMO/SOMO orbitals depicted in Fig. 5, along with HOMO-1, one can see that the oxidation takes place in the order hydrazyl anion < hydrazyl radical < hydrazine < hydrazine cation < hydrazyl cation, matching the order of the electrochemical processes in Scheme 3. Apart from contribution from the phenyl rings, all of these orbitals are located on one or both nitrogen atoms, showing the location of the oxidation processes on the hydrazine group. The calculated values of both the adiabatic and vertical energies increase in the order (1) < (2) < (3), confirming the mechanism assigned in Schemes 2 and 3. The oxidation process that takes place at the lower potential is that of the anionic hydrazyl to the hydrazyl radical,

subsequent to the abstraction of a proton from the hydrazine molecule. This has an adiabatic ionization potential of 4.62 eV. The second one is that of the hydrazyl radical, with a value of 5.26 eV, while the third value, 5.51 eV, found for the oxidation of the hydrazine molecule to the hydrazine cation, which may further lose a proton to form the hydrazil radical, should correspond to the third wave in the cyclic voltammogram, which has a very small counterpeak (EC mechanism). As these theoretical values cannot be directly correlated to the experimental voltammetric data, it is best to correlate the difference between two consecutive of these values, which is $E_a(2)-E_a(1)=0.64$ eV and $E_a(3)-E_a(2)=0.25$ eV, respectively. They agree well with the difference between two consecutive oxidation potentials, *i.e.* 0.498 V and 0.290 V. The literature data available for the diphenylpicrylhydrazyl radical in acetonitrile indicate a difference of 0.515 V²¹ between the waves assigned to the electrochemical steps (1) and (2). As seen from Table 4, the further oxidation of the two cationic species takes place at energies larger by 0.98 and 2.07 eV than the oxidation of compound B, which falls off the range of potential experimentally used.

The calculations can shed some light on the electron and spin distribution within the molecule. Density isosurfaces and spin densities mapped on density isosurfaces are presented in Fig. 6 for the radical and the cationic hydrazine. Both molecules have an excess electron density on the two central nitrogens and on the nitro groups (Fig. 6a). The trend is similar for all the species associated with compound B (data not shown). The spin is distributed on the two nitrogens, less on the NH in the case of the cation (Fig. 6b). The phenyl rings are not equivalent in what concerns the spin distribution. There is a larger excess of spin on the phenyl located anti to the pycryl fragment. Although the nitro groups have an excess of electronic density, they show only a slight excess of spin in the case of the radical, surpassed by the nitrogens and the phenyl rings. Another observation is the alternance in the spin distribution in the phenyl ring, where the carbon atoms have either an excess, or a deficit of spin (black and white isosurfaces, respectively). This is in agreement with the experimental findings for diphenylpicrylhydrazyl.²²

Table 4

Calculated ionisation potentials

Species	Oxidative step	E_v (eV)	E_a (eV)
	(1)	4.90	4.62
	(2)	5.66	5.26
	(3)	6.14	5.51
	-	6.63	6.49
	-	7.74	7.58

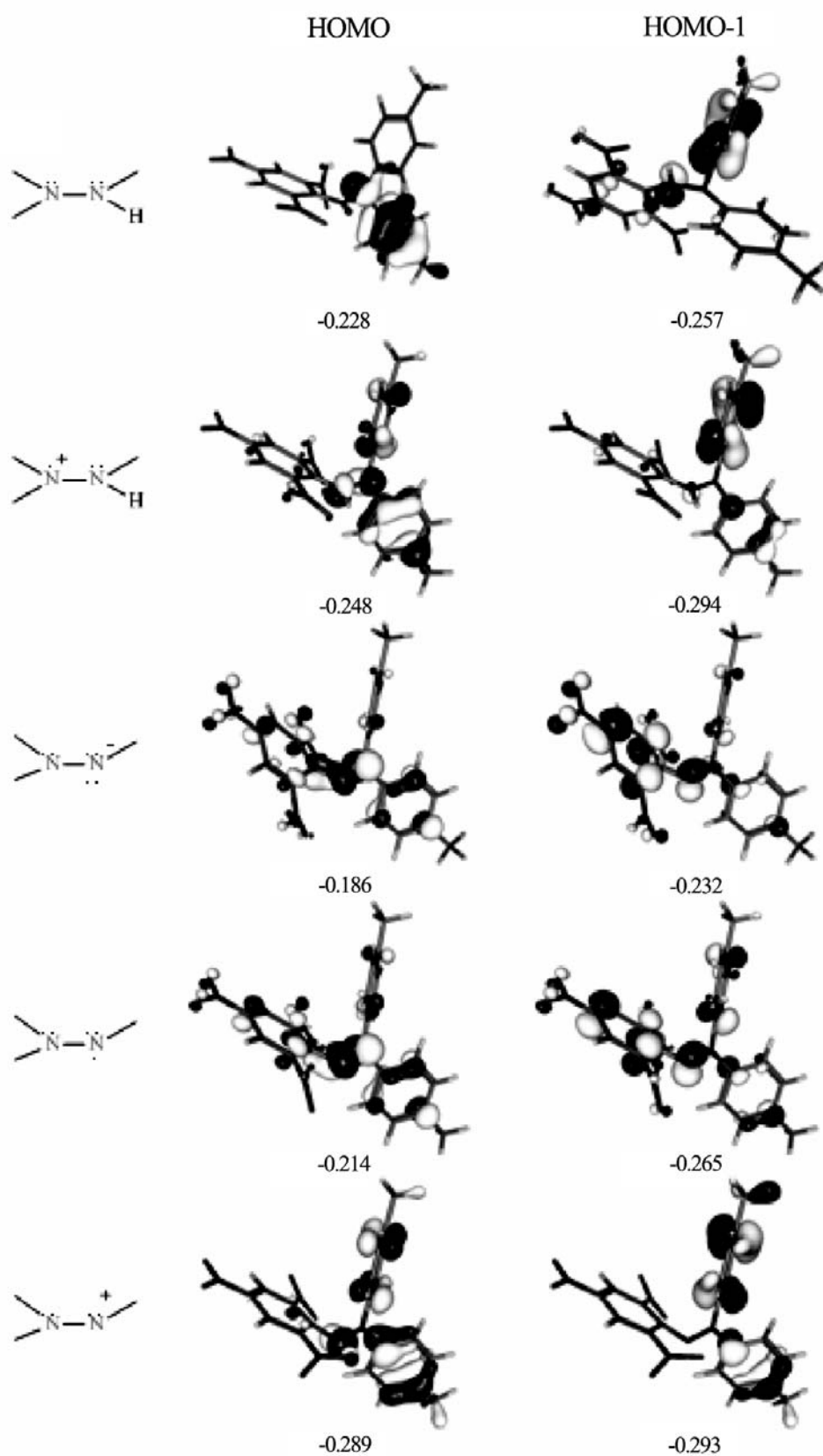
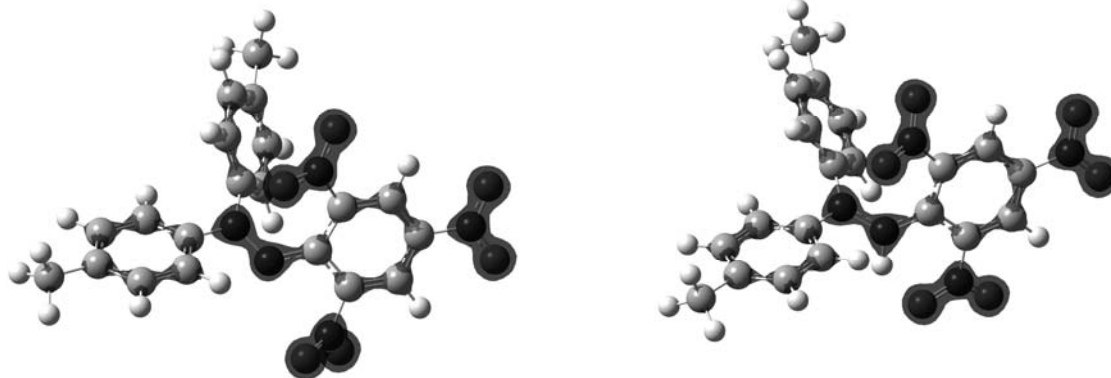


Fig. 5 – Isodensity surfaces (electronic density of 0.05 e/Bohr^3) for the molecular orbitals (last two occupied) of species considered and their energy (in eV).

a)



b)

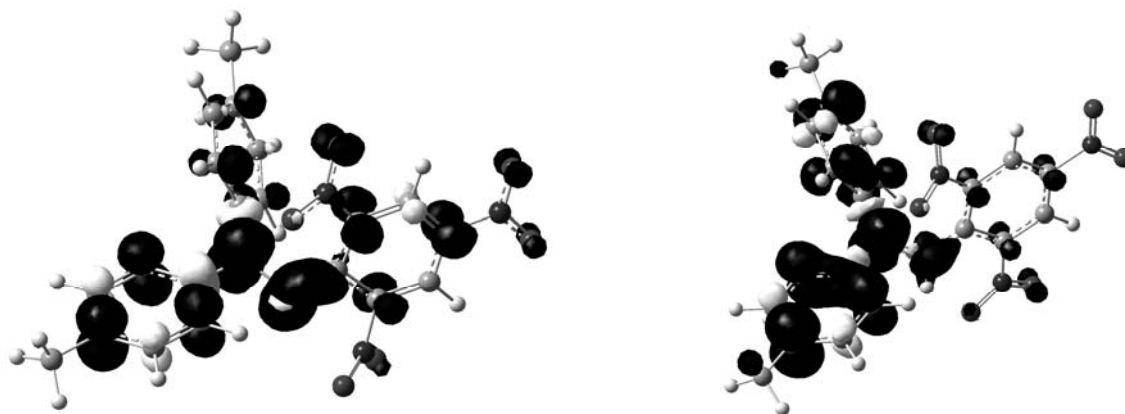


Fig. 6 – Density isosurfaces for the radical (left) and the cation (right) of compound B. a) total density 0.3 e/Bohr^3 ; b) spin density 0.002 e/Bohr^3 (black-positive; white-negative).

CONCLUSIONS

The compounds were studied using two electrochemical techniques, CV and DPV. The voltammograms obtained for different potential domains allowed finding a genetic link between the anodic and the cathodic peaks. The mechanism of the reaction that occurs at the interface electrode-solution was described studying the compounds in the absence and in the presence of methoxide ion. The electrode reactions are confined to the hydrazine moiety, N1 atom being involved in two consecutive electron transfer and N2 atom in another electron transfer which starts from the same initial compound. The presence of nitro group in position 4 and of two methyl radicals in position 4' and 4'' influences the reactivity. Enriching the solutions with basic media a cathodic shift of the anodic peak potentials for both compounds was recorded. The DPV technique was used to precisely find the peak potentials in order to justify the interpretation of the mechanism and to account for the influence of the electronic effects of nitro group vs.

trifluoromethyl group on one hand and of the methyl groups, on the other hand. The quantum chemical calculations confirm the mechanism of the electrochemical processes proposed.

REFERENCES

1. L. Catala and P. Turek, *J. Chim. Phys. et de Physico-Chimie Biologique*, **1999**, *96*, 1551.
2. N. L. Frank, R. Clérac, J.-P. Sutter, N. Daro, O. Kahn, C. Coulon, M. T. Green, S. Golhen and L. Ouahab, *J. Am. Chem. Soc.*, **2000**, *122*, 2053.
3. R. Ziessel, G. Ulrich, R. C. Lawson and L. Echegoyen, *J. Mater. Chem.*, **1999**, *9*, 1435.
4. K. Hamachi, T. I. Matsuda and H. Iwamura, *Bull. Chem. Soc. of Jpn.*, **1998**, *71*, 2937.
5. S. Goldschmidt and K. Renn, *Ber.*, **1922**, *55*, 628.
6. P. Ionita, *Lett. Org. Chem.*, **2008**, *5*, 42.
7. O. Yukowa, and T. Nakajima, *Int. J. Radiation Biol.*, **1999**, *75*, 1189.
8. M. M. Chen, K. V. Sane, R.I. Walter and J.A. Weil, *J. Phys. Chem.*, **1961**, *65*, 713.
9. C. C. Andrei, D. Bala and C. Mihailciuc, *Rev. Roum. Chim.*, **2013**, *58*, 399.
10. P. Ionita, M. T. Caproiu, C. Luca, T. Constantinescu, H. Caldararu and A. T. Balaban, *J. Label. Cpd. Radiopharm.*, **1998**, *XLI*, 791.

11. P. Ionita, T. Constantinescu, H. Caldararu, G. Ionita and M. T. Caproiu, *Rev. Roum. Chim.*, **2001**, *46*, 363.
12. Gaussian 09, M. J. Frisch, G. W. Trucks, H. B. Schlegel, G. E. Scuseria, M. A. Robb, J. R. Cheeseman, G. Scalmani, V. Barone, B. Mennucci, G. A. Petersson, H. Nakatsuji, M. Caricato, X. Li, H. P. Hratchian, A. F. Izmaylov, J. Bloino, G. Zheng, J. L. Sonnenberg, M. Hada, M. Ehara, K. Toyota, R. Fukuda, J. Hasegawa, M. Ishida, T. Nakajima, Y. Honda, O. Kitao, H. Nakai, T. Vreven, J. A. Montgomery, Jr., J. E. Peralta, F. Ogliaro, M. Bearpark, J. J. Heyd, E. Brothers, K. N. Kudin, V. N. Staroverov, R. Kobayashi, J. Normand, K. Raghavachari, A. Rendell, J. C. Burant, S. S. Iyengar, J. Tomasi, M. Cossi, N. Rega, J. M. Millam, M. Klene, J. E. Knox, J. B. Cross, V. Bakken, C. Adamo, J. Jaramillo, R. Gomperts, R. E. Stratmann, O. Yazyev, A. J. Austin, R. Cammi, C. Pomelli, J. W. Ochterski, R. L. Martin, K. Morokuma, V. G. Zakrzewski, G. A. Voth, P. Salvador, J. J. Dannenberg, S. Dapprich, A. D. Daniels, Ö. Farkas, J. B. Foresman, J. V. Ortiz, J. Cioslowski, and D. J. Fox, Gaussian, Inc., Wallingford CT, 2009.
13. A.D. Becke, *J. Chem. Phys.*, **1993**, *98*, 5648.
14. P.J. Stephens, F.J. Devlin, C.F. Chabalowski and M.J. Frisch, *J. Phys. Chem.*, **1994**, *98*, 11623.
15. A. Schaefer, C. Huber and R. Ahlrichs, *J. Chem. Phys.*, **1994**, *100*, 5829.
16. J. Tomasi, B. Mennucci and R. Cammi, *Chem. Rev.*, **2005**, *105*, 2999.
17. Y. Zhao, F. G. Bordwell, J.-P. Cheng and D. Wang, *J. Am. Chem. Soc.*, **1997**, *119*, 9125.
18. M. Hillebrand and M. Raileanu, *Rev. Roum. Chim.*, **1974**, *19*, 1227.
19. F. G. Bordwell and W. Z. Liu, *J. Am. Chem. Soc.*, **1996**, *118*, 10819.
20. Y. Zhao, F. G. Bordwell, J. P. Cheng and D. Wang, *J. Am. Chem. Soc.*, **1997**, *119*, 9125.
21. E. Solon and A. J. Bard, *J. Am. Chem. Soc.*, **1964**, *86*, 1926; *Monatshefte für Chemie*, 1983, *114*, 1035-1043.
22. J.X. Boucherle, B. Gillon, J. Maruani and J. Schweizer, *Mol. Phys.*, **1987**, *60*, 1121-1142.

